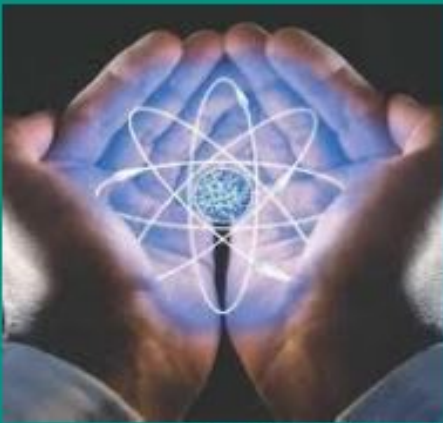


Table Of Content

Journal Cover	2
Author[s] Statement	3
Editorial Team	4
Article information	5
Check this article update (crossmark)	5
Check this article impact	5
Cite this article	5
Title page	6
Article Title	6
Author information	6
Abstract	6
Article content	8

Academia Open



By Universitas Muhammadiyah Sidoarjo

Originality Statement

The author[s] declare that this article is their own work and to the best of their knowledge it contains no materials previously published or written by another person, or substantial proportions of material which have been accepted for the published of any other published materials, except where due acknowledgement is made in the article. Any contribution made to the research by others, with whom author[s] have work, is explicitly acknowledged in the article.

Conflict of Interest Statement

The author[s] declare that this article was conducted in the absence of any commercial or financial relationships that could be construed as a potential conflict of interest.

Copyright Statement

Copyright © Author(s). This article is published under the Creative Commons Attribution (CC BY 4.0) licence. Anyone may reproduce, distribute, translate and create derivative works of this article (for both commercial and non-commercial purposes), subject to full attribution to the original publication and authors. The full terms of this licence may be seen at <http://creativecommons.org/licenses/by/4.0/legalcode>

Academia Open

Vol 10 No 1 (2025): June (In Progress)

DOI: 10.21070/acopen.10.2025.10753 . Article type: (Microbiology)

EDITORIAL TEAM

Editor in Chief

Mochammad Tanzil Multazam, Universitas Muhammadiyah Sidoarjo, Indonesia

Managing Editor

Bobur Sobirov, Samarkand Institute of Economics and Service, Uzbekistan

Editors

Fika Megawati, Universitas Muhammadiyah Sidoarjo, Indonesia

Mahardika Darmawan Kusuma Wardana, Universitas Muhammadiyah Sidoarjo, Indonesia

Wiwit Wahyu Wijayanti, Universitas Muhammadiyah Sidoarjo, Indonesia

Farkhod Abdurakhmonov, Silk Road International Tourism University, Uzbekistan

Dr. Hindarto, Universitas Muhammadiyah Sidoarjo, Indonesia

Evi Rinata, Universitas Muhammadiyah Sidoarjo, Indonesia

M Faisal Amir, Universitas Muhammadiyah Sidoarjo, Indonesia

Dr. Hana Catur Wahyuni, Universitas Muhammadiyah Sidoarjo, Indonesia

Complete list of editorial team ([link](#))

Complete list of indexing services for this journal ([link](#))

How to submit to this journal ([link](#))

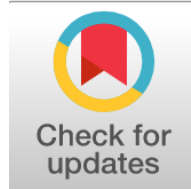
Academia Open

Vol 10 No 1 (2025): June (In Progress)

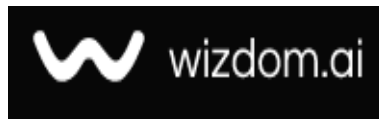
DOI: 10.21070/acopen.10.2025.10753 . Article type: (Microbiology)

Article information

Check this article update (crossmark)



Check this article impact (*)



Save this article to Mendeley



(*) Time for indexing process is various, depends on indexing database platform

Antibacterial activity of Fe₂O₃/MgO Nanoparticles against *Escherichia coli* isolated from contaminated Water

Aktivitas Antibakteri Nanopartikel Fe₂O₃/MgO terhadap Escherichia coli yang diisolasi dari Air yang terkontaminasi

Ali A. Fayyadh, alia224@uowasit.edu.iq, (1)

Ministry of Education, General Directorate of Wasit Education, Wasit, Iraq

Jawad N. K. Makassees, jawad@gmail.com, (0)

Ministry of Education, General Directorate of Wasit Education, Wasit, Iraq

Ali K. Hattab, ali@gmail.com, (0)

Department of Physics, College of Science, University of Wasit, Wasit, Iraq

⁽¹⁾ Corresponding author

Abstract

General Background: Water contamination by pathogenic bacteria, particularly *Escherichia coli*, poses serious public health risks, necessitating the development of effective antibacterial agents. **Specific Background:** Nanoparticles synthesized via green chemistry offer an environmentally sustainable alternative for bacterial control, with metal oxide nanoparticles demonstrating promising antimicrobial properties. **Knowledge Gap:** Despite extensive research on metal oxide nanoparticles, comparative studies on Fe₂O₃ and MgO nanoparticles synthesized from *Allium sativum* extract remain limited, particularly regarding their antibacterial efficacy against *E. coli* in contaminated water. **Aims:** This study investigates the antibacterial activity and characterization of Fe₂O₃ and MgO nanoparticles synthesized via a green synthesis method using *Allium sativum* extract, evaluating their efficacy against *E. coli* isolates. **Results:** Characterization via X-ray Diffraction (XRD), Transmission Electron Microscopy (TEM), and Fourier Transform Infrared Spectroscopy (FTIR) confirmed the structural and morphological properties of the nanoparticles. Fe₂O₃ nanoparticles exhibited superior antibacterial activity, generating 20 mm inhibition zones compared to MgO's 12-15 mm zones, attributed to their smaller size (24.41 nm), amorphous nature, and increased surface area. **Novelty:** This study highlights the potential of *Allium sativum*-mediated Fe₂O₃ nanoparticles as a more effective antibacterial agent than MgO nanoparticles. **Implications:** These findings support the application of green-synthesized metal oxide nanoparticles in sustainable water treatment solutions, contributing to advancements in antimicrobial technology.

Highlights:

Higher Antibacterial Efficiency – Fe₂O₃ outperforms MgO in inhibition zones.
Eco-Friendly Synthesis – *Allium sativum* ensures green nanoparticle production.
Water Treatment Potential – Effective against bacterial contamination in water.

Keywords: Fe₂O₃ nanoparticles, MgO nanoparticles, antibacterial activity, green synthesis, water treatment

Published date: 2025-03-11 00:00:00

Introduction

Water contamination stands as a fundamental global health challenge because *Escherichia coli* bacterial pathogens together with other pathogens endanger human health and environmental sustainability [1]. Water treatment technology advances have not solved the problems of removing bacteria from contaminated water supplies especially, within areas that lack appropriate resources and efficient infrastructure [2]. Waterborne diseases remain a continuous threat to human health which means immediate action is required to create effective antimicrobial solutions that work efficiently and economically [3]. Water purification and pathogen control receive innovative breakthroughs through nanotechnology which advances as a promising frontier to tackle these issues [2]. Through their unique physicochemical properties metal oxide nanoparticles consisting of Fe₂O₃ and MgO have shown outstanding potential to fight bacterial growth. The unique interaction mechanisms of nanoparticles help them eliminate bacterial cells by providing comprehensive microbial control methods [4]. Metal oxide nanoparticles demonstrate antimicrobial qualities because of several important properties. Metal oxide nanoparticles possess dimensions on the nanometer scale that lead to outstanding surface area-to-volume ratio enabling better bacterial membrane contact. The unique structural characteristics of these nanoparticles lead to better microbial cell structure breakdown and penetration rate [5,6]. The nanoparticles create reactive oxygen species (ROS) that lead to bacterial cell integrity breakdown alongside oxidative stress [4]. Nanoparticle manufacturing through conventional methods uses severe chemical procedures that create environmental hazards together with toxicological issues. Scientists now focus on green synthesis approaches because they present sustainable solutions [7]. The use of plant extracts, such as *Allium sativum* (garlic), offers a bio-friendly method for nanoparticle production. The plant extracts used as reducing and stabilizing agents potentially add antimicrobial functions to nanoparticles [8]. The microorganism *Escherichia coli* functions as a vital sign of contaminated water which presents a major threat to public health [9]. The existence of *E. coli* in water sources indicates the possibility of fecal contamination together with additional dangerous microbial pathogens. Water safety and protecting public health from transmission of waterborne diseases depend heavily on the development and implementation of powerful *E. coli* proliferation controls [3,4].

The study explores the antibacterial properties of Fe₂O₃ and MgO nanoparticles, which were synthesized through an environment-friendly method that used *Allium sativum* extract. The analysis of nanoparticle structure and morphology relied on XRD, TEM, and FTIR spectral analysis. The study measured both minimum inhibitory concentration (MIC) and sub-MIC values against *Escherichia coli* bacteria and their antibacterial and antibiofilm activities. The investigation shows efficiency evaluation between Fe₂O₃ and MgO nanoparticles and their antimicrobial mechanisms while providing sustainable water treatment methods for resource-constrained zones.

Methods

Materials

The precursors used for the synthesis of Fe₂O₃/MgO nanoparticles included ferric nitrate nonahydrate [Fe(NO₃)₃·9H₂O] and magnesium nitrate hexahydrate [Mg(NO₃)₂·6H₂O] were the minimum assay of Mg is 98.0% with maximum limits of impurities of Cl (0.005%), SO₄ (0.01%), Ca (0.05%), and iron Fe (0.0005%). Both chemical precursors were procured from Thomas Baker, India. The reducing and stabilizing agent, *Allium sativum* extract was obtained from fresh garlic bulbs.

Methods

Preparation of *Allium sativum* extract: *Allium sativum* was used in its freshest state. The bulbs were peeled, washed, and minced to as fine a paste as possible using a mortar and pestle. Ten milliliters of distilled water were used for one gram of garlic paste. The mixture was stirred for 10 minutes and left for another 1-2 hours with occasional stirring at room temperature. The solution was separated from insoluble materials using filter paper or cheesecloth, if necessary, by pouring the solvent through the materials into a collection vessel. The garlic extract prepared in distilled water was siphoned into sterilized dark glass bottles, and the bottles were placed in the refrigerator at 4°C for the retention of the bioactive compound.

Synthesis of Fe₂O₃ nanoparticles: In a beaker, ferric nitrate nonahydrate was dissolved in 50 ml distilled water at 25 °C under vigorous stirring at 700 rpm for 1 hour to form a clear solution, with one molar. Slowly add 50 ml of *Allium sativum* extract to the solution while continuously stirring, allowing *Allium sativum* extract to act as a reducing and stabilizing agent for ferric ions. Adjust the pH of the solution to an alkaline range (~12) by adding one molar of NaOH drop by drop, facilitating the precipitation of metal oxide. Stir the reaction mixture for 1h, maintaining the temperature at around 70-80°C. A color change into the yellowish to reddish-brown solution indicates the formation of the Fe₂O₃ nanoparticles. The precipitate was collected by centrifugation, washed several times with distilled water, and dried at 100°C for 4 hours, then calcined at 400°C for 2 hours to obtain Fe₂O₃ nanoparticles powder with a reddish-brown color.

Synthesis of MgO nanoparticles: In a separate beaker, one molar of magnesium nitrate hexahydrate solution was

prepared by dissolving the precursor in 50 ml distilled water under the same conditions (700 rpm, 25 °C, 1 hour). Similarly, 50 ml of *Allium sativum* extract was added dropwise to the prepared magnesium nitrate hexahydrate solution while continuously stirring, allowing *Allium sativum* extract to act as a reducing and stabilizing agent for ferric ions. The pH of the solution was adjusted to ~12 by adding one molar of NaOH drop by drop, facilitating the precipitation of metal oxide. Stir the reaction mixture for 1 hour, maintaining the temperature at around 70-80°C. A color change into a milky white solution indicates the formation of the MgO nanoparticles. The precipitate was collected by centrifugation, washed several times with distilled water, and dried at 100°C for 4 hours, then calcined at 700°C for 2 hours to obtain MgO nanoparticles powder with a white color.

Isolation and Identification of Bacterial Strains

Contaminated water sources were prepared in lactose broth at 37°C for 24 hrs and plated on EMB Agar. *E. coli* showed metallic green colonies from its lactose fermentation. The Gram stain showed that our samples contained rod-shaped bacteria that did not retain the stain. The tests confirmed indole and methyl red presence while showing no Voges-Proskauer or citrate usage. Our microbiological tests proved the laboratory culture's validity. The testing method helped us find *E. coli* in water properly.

Minimum Inhibitory Concentration (MIC) and sub-MIC

Dissolve Fe₂O₃ and MgO nanoparticles into sterile distilled water to make a concentration of 10 mg/mL. Make 1024 µg/mL to 1 µg/mL Dilutions of Fe₂O₃ and MgO Nanoparticles through Two-Level Plate Dilutions in a 96-well Microtiter Plate with Mueller-Hinton Broth. Set up empty wells for testing nanoparticles effects without particles. Add 20 µL of bacteria solution (McFarland standard 0.5 equivalent) into each well except the negative controls. To achieve 200 µL in each well maintain the inoculum concentration of 1.5×10⁸ CFU/mL. Incubate at 37°C for 18-20 hours. Place the resazurin dye solution of 20 µL directly into all well then run an incubation process of another 2 hours. Observe color changes: Full blue shows no growth while pink means bacterial development took place. Parts of the well turn light pink from reduced bacterial growth when amounts fall below the MIC.

Biofilm and Antibiofilm Activity

Fe₂O₃ and MgO nanoparticles tested their antibacterial effects on two *Escherichia coli* samples by studying biofilm growth. We made 1 × 10⁶ CFU/mL bacterial cultures using LB broth before incubating them at 37°C for 16-18 hours. We dissolved our nanoparticles (10-100 µg/mL) in DMSO and processed them through filters to create sterility. To create biofilms we added 100 microliters of bacterial culture to 96-well plates and kept them at 37 °C for 24 hours. The wells received plain PBS as a washing solution to remove planktonic cell samples. By placing 100 µL of Fe₂O₃ or MgO nanoparticle solutions into existing biofilms and letting them develop for a further 24 hours. Measure the biofilm amounts using 0.1% crystal violet tubes and determine absorbance at 570 nm. Identified MBIC50 as the weakest concentration of nanoparticles that successfully prevented 50% of bacterial surface accumulation. Scientists compared how effective Fe₂O₃ and MgO nanoparticles worked to stop *E. coli* growth in biofilms.

Antibacterial Activity

Using the agar well diffusion method at their MIC concentrations. The antibacterial characterization of Fe₂O₃ and MgO nanoparticles was tested against two isolated *Escherichia coli*. Allowing each bacterial culture to grow at 37°C in nutrient broth for 18-24 hours. The suspension was developed to hold 1.5 X 10⁸ CFU in 5 mL of normal saline from a single *E. coli* colony. The bacterial suspension was to dry for 10 minutes by spreading it evenly across Mueller-Hinton agar plates with a sterile cotton swab. Five millimeter wells were cut into the agar plate and we added 15 mg/ml of Fe₂O₃ or MgO nanoparticle solutions to each. The test included two wells - the first with *azithromycin* at 15 mg/ml proved positive, whereas DMSO served as our negative control. Plates were incubated at 37°C for 18 hours. The size of inhibition zones was measured after incubation to determine how effective Fe₂O₃ and MgO nanoparticles work against *E. coli*.

Characterization Techniques

Different techniques were used to analyze the synthesized Fe₂O₃/ MgO nanoparticles. The X-ray Diffraction (XRD) analysis was conducted using a PANalytical X'Pert PRO diffractometer equipped with Cu K α radiation ($\lambda = 1.54060$ Å), operated at 40 kV and 30 mA. The diffractogram was recorded in the 2 θ range from 10° to 80° with a step size of 0.02° at a scanning rate of 1°/min. The surface morphology and the particle size of the Fe₂O₃/MgO nanoparticles were investigated using a JEOL JEM-2100 Transmission Electron Microscope (TEM) at an accelerating voltage of 200 kV. A small portion of the sample was stained with ethanol, ultrasonicated, and then placed on a copper grid coated with carbon for TEM. The Morphology and size of the particles were clearly shown by analyzing the high magnification TEM images while the crystal nature of the nanoparticles was further supported by authors using selected area electron diffraction (SAED). Fourier Transform Infrared (FT-IR) spectra were obtained using a Bruker Alpha II FT-IR spectrometer in the range of (4000 to 400) cm⁻¹ at a resolution of 4 cm⁻¹. Fe₂O₃/ MgO nanoparticles were mixed with potassium bromide (KBr) to form pellets for transmission measurements. The recorded spectra were analyzed to confirm the presence of characteristic bonds of Fe₂O₃/ MgO nanoparticles, particularly the Fe-O stretching vibration.

Results and Discussion

The X-ray diffraction (XRD) technique is employed to characterize the crystal structure of the prepared samples. The Debye-Scherrer Eq 1 was used to calculate the average crystallite size. It is employed to measure the size of crystal particle fragments.

$$D = (k\lambda)/(\beta \cos \theta) \dots \dots \dots 1$$

Where D is the crystallite size (nm), K is the crystallite's dimensionless form factor (0.94), X-ray wavelength ($\lambda = 0.154060$ nm), θ is the Bragg diffraction angle (Radian), and β is the FWHM of the selected peak are all given (Radian) [10]. The X-ray diffraction (XRD) patterns of Fe₂O₃/MgO nanoparticles are shown in Fig. 1. The Fe₂O₃ nanoparticles identified a cubic crystal structure of Fe₂O₃ according to the entry crystallography open database (COD) [96-900-6318] and orthorhombic crystal structure of Fe₂O₃ according to the entry cod [96-400-2384]. The three strongest peaks (2 θ); 29.58°, 32.74°, and 48.78° correspond to planes and crystallite sizes of (013) plane: 30.60nm, (122) plane: 22.88 nm, and (142) plane: 19.74nm, respectively. On the other hand, the MgO nanoparticles identified a cubic crystal structure of MgO according to the entry crystallography open database (COD) [96-900-6474]. The three strongest peaks (2 θ); 35.72°, 42.94°, and 62.24° correspond to planes and crystallite sizes of (111) plane: 21.47 nm, (200) plane: 41.75 nm, and (202) plane: 17.19 nm, respectively [11].

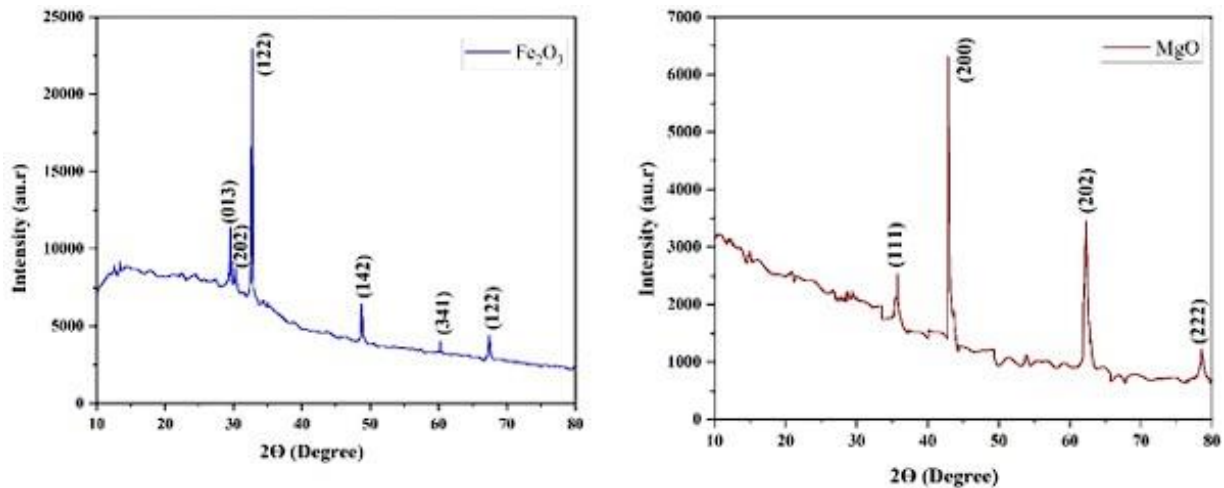


Figure 1. XRD pattern of Fe₂O₃ and MgO nanoparticles.

According to the data obtained through X-ray crystallography, it can be pointed out that on average MgO nanoparticles offer a distinct edge due to a more crystalline cubic structure and average crystallite size of 26.81 nm. For Fe₂O₃, which exists in the two phases, both the cubic and orthorhombic, with a lower crystallite size of 24.41 nm. Small crystallite sizes generally lead to large surface area-to-volume ratios, ensuring greater efficiency of interaction with bacterial cell membranes. However, the crystal structure of Fe₂O₃ is an amorphous structure meaning there could be several ways through which the Fe₂O₃ can act against bacteria through each face of the crystal, this result agrees with [12-14]. Through the analysis of TEM images of both Fe₂O₃ and MgO nanoparticles, fig. 2 identified differences in particle morphology. Further, MgO nanoparticles show an average particle size of (~47 nm) with quasi-spherical morphology round edges, relatively lower polydispersity, and comparatively less aggregation have been identified with good electron contrast thus representing epochs of their crystalline nature. Fe₂O₃ nanoparticles, however, are smaller in average particle size (~29 nm) with quasi-spherical in shape which also tend to form long chain-like clusters and branched aggregates are more pronounced, have better-defined particle perimeters and an uneven contrast that suggests variations in the thickness at the points of aggregation. The sample of Fe₂O₃ has a relatively narrow size distribution with relatively homogeneous quasi-spherical shapes with clear boundaries, while the sample of MgO has a higher variation in particle size and shapes. The degree of clustering between both elements is dissimilar with MgO having a dispersed cluster of moderate agglomeration while Fe₂O₃ has a strong clustering mile along the formation network. These morphological characteristics are in agreement with the XRD data which revealed that MgO has a bigger crystallite size than Fe₂O₃. Given that the Fe₂O₃ nanoparticles used here have a small particle size and a greater tendency to agglomerate, the particles might possess a higher surface area to volume ratio and increased active sites in contact with bacteria, which makes them most suitable for antimicrobial uses in water treatment.

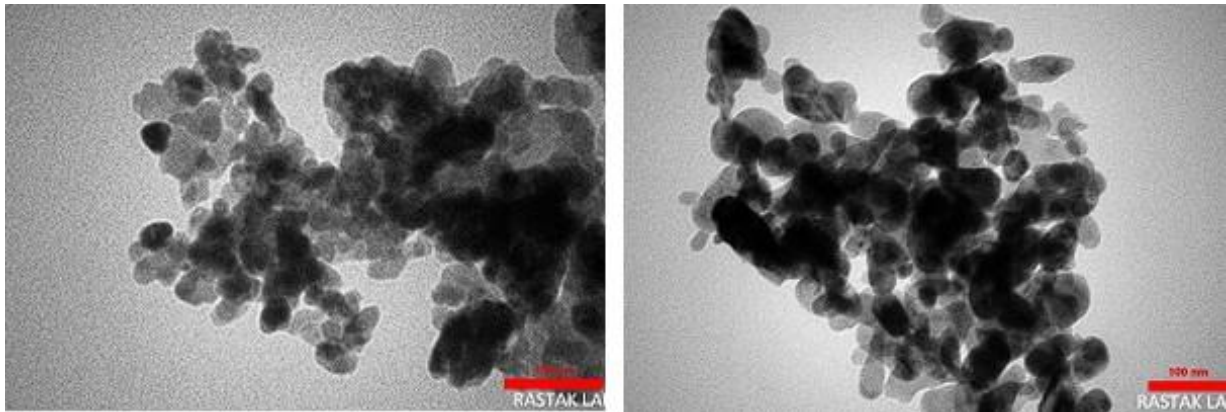


Figure 2. TEM images of (a-left) Fe_2O_3 and (b-right) MgO nanoparticles

The FTIR spectra in Fig.3 show different vibrational peaks of Fe_2O_3 and MgO nanoparticles having different chemical bonds and functional groups. In the case of Fe_2O_3 nanoparticles, the absorption peak at 3435.41cm^{-1} is attributed to the stretching of O-H groups that might be a part of hydroxyl groups present on their surface or may be due to the presence of adsorbed water molecules [13]. The peak at 1635.78cm^{-1} is assigned to H-O-H bending vibrations of the adsorbed water molecules on the surface [15]. The two absorption peaks at 1384.39cm^{-1} and 1060.76cm^{-1} are assigned to Fe-O-H bending vibrations indicating the presence of hydroxyl groups bound to iron atoms [16]. The band observed in the region 679.86cm^{-1} is assigned to Fe-O-Fe stretching vibrations of the iron oxide structure. For MgO nanoparticles, the broad absorption band appears at 3435.61cm^{-1} is refers to stretching vibrations of O-H belonging to the surface hydroxyl groups. The high intensity and narrow peak at 1634.56cm^{-1} is due to H-O-H bending vibrations of the adsorbed water molecules on the surface, while the peaks in 1384.43cm^{-1} and 1028.13cm^{-1} are assigned to Mg-O-H bending vibrations. The peak observed in the region 698.57cm^{-1} is assigned to Mg-O-Mg stretching vibrations of the magnesium oxide structure [17]. Consistent with the XRD and TEM analysis, FTIR spectra give additional information on the crystallinity and test surface of both materials. This is in agreement with the trends of agglomeration seen in the TEM images, specifically for the MgO nanoparticles where stronger particle-particle interactions were argued based on the broader Voigt profile fitting of the O-H stretching bands. The clear and sharp bands observed for metal-oxygen vibration conform with the crystalline nature confirmed by XRD, where Fe_2O_3 existed in both cubic and orthorhombic phases and the MgO existed in only a cubic phase. The spectra obtained have shown that the intensities of the peaks in the MgO sample are sharper and more intense, especially on the metal-oxygen vibration region which is an indication of better crystallinity as has been confirmed by the XRD result. Also, previous characterizations of the surface by FTIR analysis revealed the presence of hydroxyl groups which could be involved in the generation of reactive oxygen species and interaction with bacterial membranes, particularly in Fe_2O_3 . This detailed characterization shows that the microstructures established at atomic (FTIR), crystalline (XRD), and nanometer (TEM) resolutions form the basic underlying and nested architecture that gives the material its characteristics and suggests its potential antimicrobial functionality.

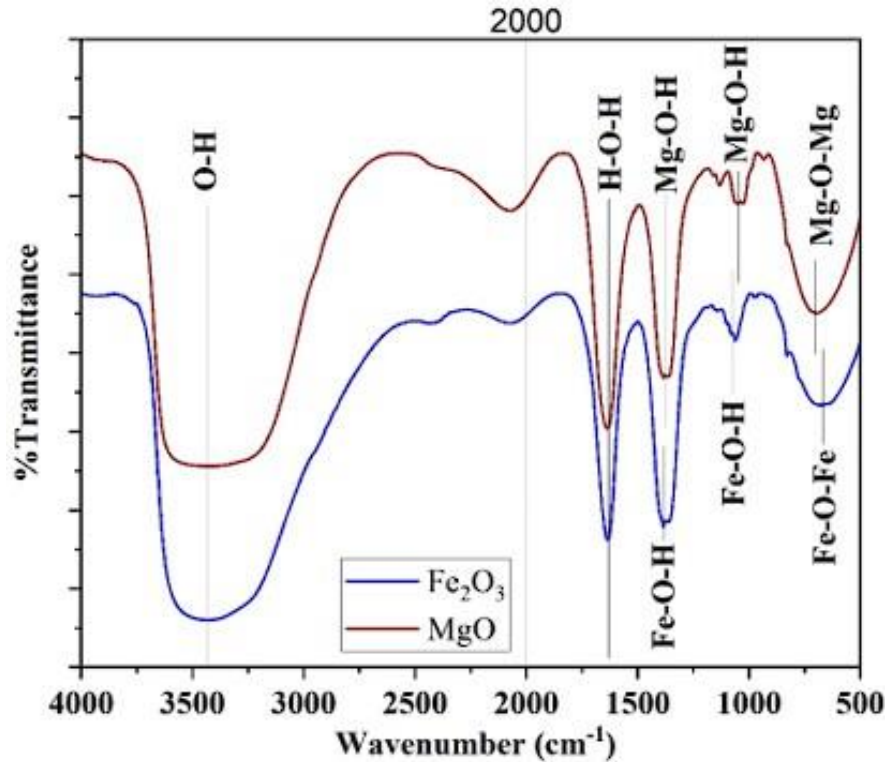


Figure 3. FTIR spectra of Fe₂O₃ and MgO nanoparticles.

Isolation Efficiency and Bacterial Identification Outcomes

Colony Morphology Isolates metallic green sheen on EMB agar, and pink on MacConkey agar. Gram Staining all isolates Gram-negative rods observed under the microscope. Biochemical Tests Isolates Indole-positive, Methyl Red-positive, Voges-Proskauer-negative, Citrate-negative. All isolates were successfully identified as *Escherichia coli* based on colony morphology, Gram staining, and biochemical tests. This confirms contamination by *E. coli* in the water sample.

MIC and sub-MIC Evaluation and Antibacterial Activity

Table 1 represents the Minimum Inhibitory Concentration (MIC) and sub-MIC evaluations of Fe₂O₃ and MgO nanoparticles. The susceptibility levels of Fe₂O₃ Nanoparticles differ between the two tested bacterial isolates. *E. coli 1* displays stronger antimicrobial properties with 8 µg/ml as MIC while its sub-MIC corresponds to 4 µg/ml. The MIC value of *E. coli 2* reaches 32 µg/ml whereas its sub-MIC reaches 6 µg/ml so this isolate reacts differently to the substance. The small crystallite dimension of Fe₂O₃ at 24.41 nm together with its amorphous structure allows numerous reactive sites which bacteria use for interaction. The structural characteristics that lead to increased aggregation and chain-like clustering diminish the ability of Fe₂O₃ nanoparticles to spread uniformly as well as reach bacterial membranes directly. The increased surface area-to-volume ratio along with ROS generation capacity which shows evidence through FTIR detection of hydroxyl groups enables Fe₂O₃ nanoparticles to be usable in applications that require water treatment. The MgO nanoparticles present stable antimicrobial action against *E. coli* isolates with MIC at 32 µg/ml and sub-MIC at 16 µg/ml for both test strains. The antimicrobial properties remain consistent because XRD and TEM data show that these nanoparticles possess large crystallite dimensions (26.81 nm) with pure cubic crystalline structure and quasi-spherical morphology. The nanostructured properties decrease aggregation while enhancing dispersion which leads to equal bacterial membrane interactions. FTIR spectral data confirm that MgO exhibits higher crystalline quality indicated by its sharper metal-oxygen vibration peaks since this typically leads to stability and better interaction performance. Aside from ROS generation, the antimicrobial properties of MgO are increased because of the hydroxyl groups that exist on its surface.

Table 1. MIC and sub-MIC of Fe₂O₃ and MgO nanoparticles

Isolates	Fe ₂ O ₃ nanoparticles(µg/ml)		MgO nanoparticles (µg/ml)	
	MIC	Sub-MIC	MIC	Sub-MIC
E.coli 1	8	4	32	16
E.coli 2	32	6	32	16

Evaluation of Antibacterial Activity

Antibacterial evaluations of Fe₂O₃ and MgO nanoparticles versus E. coli isolates can be observed in Table 2 and Figure 4 thus proving their ability to act as antimicrobial agents. The antibacterial studies demonstrate the strong antibacterial behavior of Fe₂O₃ nanoparticles because they produced inhibition zones of 20 mm which were equal for both E. coli 1 and E. coli 2. Their antibacterial activity excels due to their small particle dimensions which provide an elevated surface area-to-volume ratio together with reactive functional groups even though they display amorphous structure-based aggregation.

Table 2. Antibacterial activity of Fe₂O₃ and MgO nanoparticles.

The bacterial isolates	The diameter of the inhibition zone (mm)		
	Fe ₂ O ₃ nanoparticles (15 mg/ml)	MgO nanoparticles (15 mg/ml)	Azithromycin (15 mg/ml)
E.coli 1	20	15	8
E.coli 2	20	12	7

The antibacterial activities of MgO nanoparticles produce inhibition zones reaching 15 mm against *E. coli 1* and 12 mm against *E. coli 2*. The antibacterial properties of Fe₂O₃ nanoparticles stem from their big crystallite dimensions and cubic structure along with decreased particle aggregation while showing less efficiency than Fe₂O₃. Azithromycin achieves minimal antibacterial activity which results in 8 mm inhibition zones for *E. coli 1* and 7 mm for *E. coli 2* due to its reduced interaction with microorganisms when compared to both nanoparticles.



Figure 4. Antibacterial activity of Fe₂O₃ and MgO nanoparticles.

Conclusion

The study showed that Fe₂O₃ /MgO nanoparticles synthesized from *Allium sativum* extract proved significantly effective against *E. coli* bacterial isolates. Study outcomes delivered fundamental knowledge about how nanoparticles functioned and were structured. The Fe₂O₃ nanoparticles demonstrated superior antibacterial action as they had smaller dimensions, an amorphous arrangement, and a greater surface area-to-volume ratio, which facilitates enhanced interaction with bacterial membranes. XRD, TEM, and FTIR spectroscopic analyses revealed different morphological characteristics of the examined nanoparticles. The aggregation pattern of Fe₂O₃ nanoparticles was higher than the distributed quasi-spherical structure of MgO nanoparticles. The antibacterial performance of Fe₂O₃ nanoparticles exceeded that of MgO nanoparticles because Fe₂O₃ nanoparticles created 20 mm inhibition zones while MgO nanoparticles produced smaller 12-15 mm inhibitory zones. The study evidence demonstrates that nanoparticles, especially Fe₂O₃ display useful water treatment capabilities. Nanoparticle production benefits from environmental safety due to the green synthesis technique derived from *Allium sativum* extract. The advancement of future research must focus on optimizing production methods for nanoparticles while extending antimicrobial assessment and developing industrial water treatment solutions based on this approach.

References

1. B. M. Mustafa and N. E. Hassan, "Water Contamination and Its Effects on Human Health: A Review," *J. Geogr. Environ. Earth Sci. Int.*, vol. 28, no. 1, pp. 38–49, 2024.
2. D. B. Olawade et al., "Nanoparticles for Microbial Control in Water: Mechanisms, Applications, and Ecological Implications," *Front. Nanotechnol.*, vol. 6, p. 1427843, 2024.
3. S. Elhenawy et al., "Emerging Nanomaterials for Drinking Water Purification: A New Era of Water Treatment Technology," *Nanomaterials*, vol. 14, no. 21, p. 1707, 2024.
4. P. M. de Souza, A. K. Mahapatra, and E. P. da Silva, "Emerging Technologies for Water Decontamination: Ensuring Safe and Clean Water," in *Emerging Trends and Technologies in Water Management and Conservation*, 1st ed., vol. 1, 2025, pp. 35–86.
5. D. B. Olawade et al., "Nanoparticles for Microbial Control in Water: Mechanisms, Applications, and Ecological Implications," *Front. Nanotechnol.*, vol. 6, p. 1427843, 2024.
6. D. Dey, S. Chowdhury, and R. Sen, "Insight Into Recent Advances on Nanotechnology-Mediated Removal of Antibiotic Resistant Bacteria and Genes," *J. Water Process Eng.*, vol. 52, p. 103535, 2023.
7. S. H. Khan, "Green Nanotechnology for the Environment and Sustainable Development," in *Green Materials for Wastewater Treatment*, 1st ed., 2020, pp. 13–46.
8. N. T. T. Nguyen et al., "Formation, Antimicrobial Activity, and Biomedical Performance of Plant-Based Nanoparticles: A Review," *Environ. Chem. Lett.*, vol. 20, no. 4, pp. 2531–2571, 2022.
9. J. D. Van Elsas et al., "Survival of Escherichia Coli in the Environment: Fundamental and Public Health Aspects," *ISME J.*, vol. 5, no. 2, pp. 173–183, 2011.
10. K. Mongkolsuttirat and J. Buajarern, "Uncertainty Evaluation of Crystallite Size Measurements of Nanoparticle Using X-Ray Diffraction Analysis (XRD)," *J. Phys.: Conf. Ser.*, vol. 1719, no. 1, 2021.
11. O. A. Bulavchenko and Z. S. Vinokurov, "In Situ X-Ray Diffraction as a Basic Tool to Study Oxide and Metal Oxide Catalysts," *Catalysts*, vol. 13, no. 11, p. 1421, 2023.
12. P. K. Stoimenov et al., "Metal Oxide Nanoparticles as Bactericidal Agents," *Langmuir*, vol. 18, no. 17, pp. 6679–6686, 2002.
13. M. Arakha et al., "Antimicrobial Activity of Iron Oxide Nanoparticle Upon Modulation of Nanoparticle-Bacteria Interface," *Sci. Rep.*, vol. 5, no. 1, p. 14813, 2015.
14. J. Jiang, G. Oberdörster, and P. Biswas, "Characterization of Size, Surface Charge, and Agglomeration State of Nanoparticle Dispersions for Toxicological Studies," *J. Nanoparticle Res.*, vol. 11, pp. 77–89, 2009.
15. R. M. Cornell and U. Schwertmann, *The Iron Oxides: Structure, Properties, Reactions, Occurrences, and Uses*, 2nd ed. Weinheim, Germany: Wiley-VCH, 2003.
16. F. Paladini et al., "Surface Chemical and Biological Characterization of Flax Fabrics Modified With Silver Nanoparticles for Biomedical Applications," *Mater. Sci. Eng. C*, vol. 52, pp. 1–10, 2015.
17. P. K. Stoimenov et al., "Metal Oxide Nanoparticles as Bactericidal Agents," *Langmuir*, vol. 18, no. 17, pp. 6679–6686, 2002.